Eng. Sci., 2020, 10, 24–34

Engineered Science

DOI: https://dx.doi.org/10.30919/es8d1008

Graphitic Carbon Nitride: Preparation, Properties and Applications in Energy Storage

Wen Zhao, Zhaoqian Yan, and Lei Qian*

Abstract

Graphitic carbon nitride (g-C_3N_4) has received much attention in recent years due to its unique optical and electrochemical properties. In this review, preparation, properties and some applications of g-C_3N_4 in energy storage are summarized. In order to improve the specific surface area of g-C_3N_4, hard and soft template, template-free and exfoliation methods are usually used. The properties of g-C_3N_4 including stability, optical, photoelectrochemical and electrochemical properties are introduced. Some applications in photocatalysis, electrocatalysis and Li-based batteries are also analyzed. Finally, the outlook of g-C_3N_4 is also provided.

Keywords: g-C_3N_4; Synthesis; Properties; Applications.
Received date: 1 March 2020; Accepted date: 11 May 2020
Article type: Review article

1. Introduction

The growing population and rising consumption of fossil fuels continuously increase the people's awareness in energy requirement and environment damage. At present, the large demand of fossil fuels has caused environmental damages. Therefore, certain solutions need to be raised to promote sustainable energy storage technologies towards urgent energy demands. Novel nanomaterials are considered as the efficient way to address the problems.[1] Various kinds of nanomaterials with special properties have been prepared and used for energy conversion and storage. Nanostructured carbon nitrides (CNs) are promising in terms of a variety of applications. CNs can be synthesized by the pyrolysis of nitrogen rich precursors. Depending on the degree of condensation, the resulting materials are called melon (linear polymers of connected tri-s-triazines via secondary nitrogen) or graphitic carbon nitrides (g-C_3N_4, 2D sheets of tri-s-triazine connected via tertiary amines). g-C_3N_4 is considered to be the most stable allotrope of various CN structures because of its favorable intriguing properties such as high hardness, facile preparation, unique structure and chemical stability.[1-7] Two structures have been proposed as the basic building block of g-C_3N_4.[8] One is composed of condensed s-triazine units (ring of C_3N_3) with a periodic array of single carbon vacancies; the other is composed of condensed tri-s-triazine (triring of C_6N_7) subunits connected through planar tertiary amino groups with larger periodic vacancies in the lattice.[8] The second one is the most stable local connection pattern.[9,10] Therefore, tri-s-triazine is widely accepted as the basic unit for the g-C_3N_4. As a result, g-C_3N_4 has a great potential in energy conversion and storage as well as environmental applications,[11] such as photocatalysis,[12,13] fuel cells,[14,15] CO_2 capture,[16,17] and battery catalysis.[18,19]

g-C_3N_4 is a visible-light-response material (2.7 eV bandgap), and the energy position of conduction band (CB) and valence band (VB) is at -1.1 and 1.6 eV vs. normal hydrogen electrode (NHE), respectively. In addition, g-C_3N_4 has very high resistance to heat, strong acid, as well as strong alkaline solution. g-C_3N_4 contains carbon and nitrogen elements only and it can be synthesized from the facile pyrolysis of nitrogen-rich precursors, such as melamine,[20,21] urea,[22,23] thiourea[24,25] and cyanamide.[26,27] It has been reported that the choice of precursor and different pyrolysis temperatures have great influences on the electronic structure and bandgap of g-C_3N_4, which will further influence its potential applications in many fields.[25-30] Recently, some significant advances have been made regarding the research of g-C_3N_4. Therefore, an article which can summarize the synthesis of g-C_3N_4-based materials and their potential

Key Laboratory for Liquid-Solid Structural Evolution and Processing of Materials (Ministry of Education), Shandong University, 17923 Jingshi Road, Jinan 250061, China.
E-mail: qleric@sdu.edu.cn

applications in energy storage is necessary.

This review article focuses on recent progress in the properties, synthesis and potential applications of g-C_3N_4 and g-C_3N_4-based nanocomposites in energy storage and conversion, such as photocatalytic hydrogen evolution, oxygen reduction reaction (ORR), and Li-based battery. Eventually, some concluding remarks and perspectives on current situations of the g-C_3N_4-related studies are presented, which are aimed to improve the understanding as well as promote the applications of g-C_3N_4-based nanocomposites. Therefore, this review gives a brief summary of synthesis, properties and applications of g-C_3N_4 and its composites.

2. Preparation of g-C_3N_4 materials

g-C_3N_4 contains C and N elements only and it is a stable polymer semiconductor. At present, many nitrogen-rich organic precursors (such as urea, melamine, dicyandiamide, thiourea and cyanamide) are used for preparing g-C_3N_4. However, carbon nitride materials prepared by direct condensation of these precursors are with bulk structures, which have low specific surface areas. For practical applications as catalysts, it is necessary to introduce well-controlled porous structures in the bulk g-C_3N_4. Researchers have designed several different methods to obtain porous g-C_3N_4.

2.1 Hard and soft-template method

"Templating" essentially involves the replication of one structure into another under the structural inversion. A template, in its most general definition, is a structure-directing agent. Template method therefore is a versatile technique for the preparation of nanostructured or porous materials, as the size and shape of the resulting pore structures can be easily tuned by the appropriate template.[28]

The hard templates are used to fabricate porous structures and design hierarchical pore architectures in g-C_3N_4.[4,29,30] Silica templates are used as the typical structure directing agent to control the nanostructures. Groenewolt *et al.*[31] reported on synthesis of novel g-C_3N_4 nanoparticles with different diameters by employing different pore size mesoporous silica matrices. Afterwards, many researches on mesoporous g-C_3N_4 materials prepared by silica-based hard templates have been reported. Highly ordered mesoporous g-C_3N_4 with tunable pore diameters was synthesized by using aminoguanidine hydrochloride as precursor and SBA-15 as hard templates.[32] Fukasawa *et al.*[33] used uniform-sized silica nanospheres as templates to synthesize ordered porous g-C_3N_4. Xu *et al.*[34] employed guanidinium chloride as precursors to synthesize mesoporous g-C_3N_4 by a nanocasting method. The as-prepared g-C_3N_4 samples possessed two types of pores and high specific surface areas. Park *et al.*[35] prepared 2-dimensional (2D) and 3-dimensional (3D) mesostructured g-C_3N_4 via the incipient wetness process with mesoporous silica as a hard template. These materials exhibit open pores and large specific surface area. Notably, in the hard-template approach, the removal of the template is necessary to obtain the desired g-C_3N_4 structure. This process usually involves aqueous NH_4HF_2 or HF, which may cause damages to the environment.

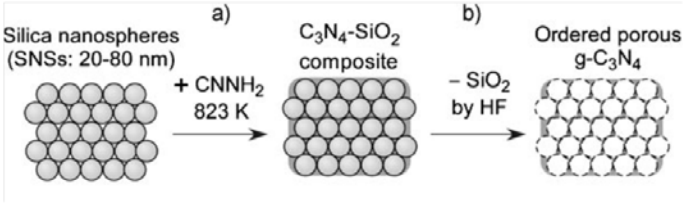

Fig. 1 Schematic illustration of the synthesis of ordered porous g-C_3N_4 by using close-packed silica nanospheres (SNSs) as the primary template. Reproduced with permission[33] (Copyright © 2010, John Wiley and Sons)

By contrast, the soft-template method is greener, since the soft template can be removed by calcination. In the soft-template method, the mesopores of g-C_3N_4 are achieved by amphiphilic surfactant molecules driven by the natural tendency of reducing interfacial energy.[1] Therefore, the properties of organic templates are vital for the mesostructures of g-C_3N_4 materials and the templates are called structure directing agents. The soft-template process can fabricate g-C_3N_4 with different morphologies by changing the soft templates as well as simplify the preparation of g-C_3N_4. Many researchers have used different surfactants such as P123, Triton X-100, Brij30 and Brij58 or liquids as soft templates to prepare g-C_3N_4 with different morphologies and specific surface areas. For example, Yan *et al.*[36] used Pluronic P123 as soft-templates to prepare g-C_3N_4 with worm-like pore, which possessed high BET surface. Yang *et al.*[37] prepared mesoporous g-C_3N_4 by a soft template of Triton X-100. The hydrophobic groups of this template can form bubbles during the synthesis of mesoporous g-C_3N_4. In the preparation of 3D porous sulfur/graphene@g-C_3N_4 (S/GCN) hybrid sponge, oil emulsion droplets were used to form pores, and 3D interlinked S/GCN sponge structure through the hydrothermal process was achieved.[40]

(Fig. 2) presents two representative synthesis routes for ordered mesoporous materials, which are suitable for the preparation of g-C_3N_4.[38]

The hard-template method has the advantage that the copies of the template structure can be achieved easily. A variety of inorganic nanostructures can be used as templates for the synthesis of organic replicas.[28] The soft-template method is more environmental-friendly. However, the improper choice of template and pyrolysis can result in unsuccessful synthesis of g-C_3N_4, since the template materials will be decomposed before the formation of g-C_3N_4. Moreover, the template will leave carbon residue in the final products, which could decrease the nitrogen content and lower its catalytic activity.[1]

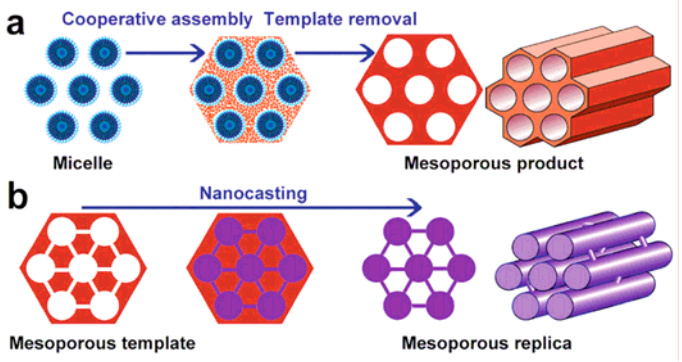

Fig. 2 Scheme of two representative synthesis routes for ordered mesoporous materials: (a) soft-templating method and (b) hard-templating (nanocasting) method. Reproduced from [38] with permission from The Royal Society of Chemistry.

2.2 Template-free method

Han *et al.*[38] prepared porous g-C_3N_4 by a facile thermal-treatment of dicyandiamide. The prepared porous g-C_3N_4 achieved a high BET surface area (201-209 m^2 g^{-1}) and large pore volume (0.50-0.52 m^3 g^{-1}). Tahir *et al.*[39] prepared g-C_3N_4 nanofibers (GCNNFs) by a facile template-free method. Melamine reacted with ethanol first and then was annealed at 450 °C for 2 hours to get GCNNFs, which exhibited 1D structure with a high specific surface area. Graphene modified porous g-C_3N_4 (porous g-C_3N_4/graphene) was also synthesized by the thermal calcinations.[40] In this method, the polymerization process was carried out at different temperatures, and the porous g-C_3N_4 was obtained at high calcination temperatures.

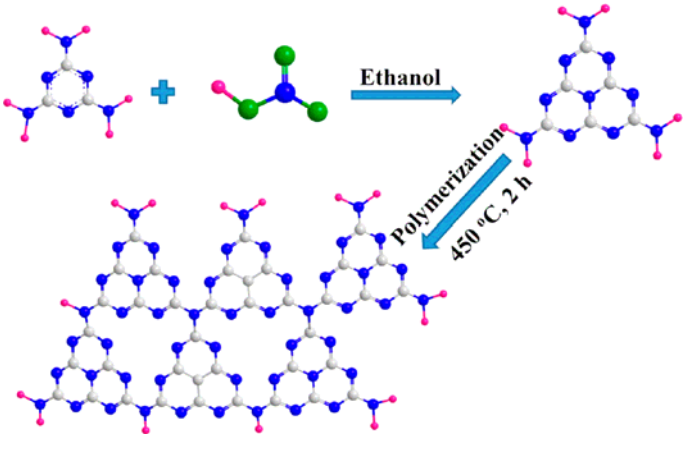

Fig. 3 Schematic representation of chemical reaction for the synthesis of GCNNF. Reproduced with permission[40] (Copyright © 2014, American Chemical Society)

For both the hard-template and soft-template methods, the complete removal of the template may require complicated post-treatments and be very challenging. Therefore, it is necessary to develop a template-free method. Such template-free method does have the advantage that it is one-step processes. Any template synthesis and removal thus can be avoided, and no waste is produced. The choice of precursor is vital for the template-free method, so the research focus mostly concentrates on the kinds of precursor as well as the changes of thermal treatment.

2.3 Exfoliation of bulk g-C_3N_4

2D g-C_3N_4 sheets show a unique layered structure and they can be prepared by the exfoliation of bulk g-C_3N_4. Li *et al.*[20] obtained macroscopic foam-like holey ultrathin g-C_3N_4 nanosheets (CNHS) by a long-time thermal treatment of bulk g-C_3N_4 in air (Fig. 4). Holey 2D layered structure of CNHS has a large surface area and can provide more active sites for catalytic reaction (Fig.5). Besides, this unique structure of CNHS favors the electron movement. She *et al.*[41] synthesized 2D graphene-like g-C_3N_4 by liquid exfoliation of bulk g-C_3N_4. The obtained g-C_3N_4 exhibits a 2D layer structure, a high specific surface area, which can promote both electron transport and photocatalytic activity.

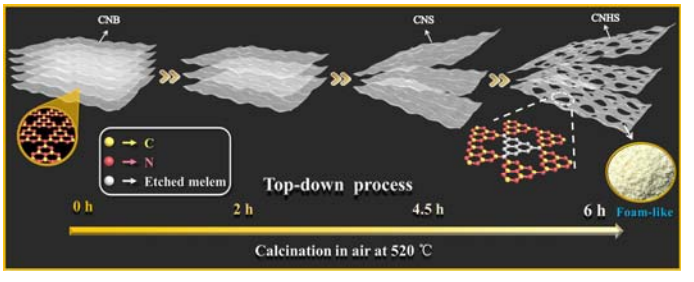

Fig. 4 Top-down process for preparation of foam-like holey ultrathin g-C_3N_4 nanosheets. Reproduced with permission[20] (Copyright@ 2016, WILEY-VCH Verlag GmbH & Co. KGaA, Weinheim)

3. Properties of g-C_3N_4 materials

3.1 Stability

3.1.1 Thermal stability

According to the research of Yan *et al.*,[21] g-C_3N_4 started to decompose at the temperature of 600 °C. Fig. 6 shows the thermogravimetric-differential scanning calorimetry analysis of melamine and g-C_3N_4. It was clear that g-C_3N_4 started to decompose when the temperature increased to 600 °C, and g-C_3N_4 decomposed completely when the heating temperature reached 750 °C. The thermal stability of g-C_3N_4 is one of the highest among inorganic materials. The thermal stability of g-C_3N_4 is affected by different preparation methods and the choice of precursors.[6,42-46]

The thermal stability of g-C_3N_4 somewhat varies from different polymerization degrees of g-C_3N_4 in different preparation methods. For example Cui *et al.*[44] synthesized bulk g-C_3N_4 by direct thermal polymerization of ammonium thiocyanate as the precursor. Then nanostructured g-C_3N_4

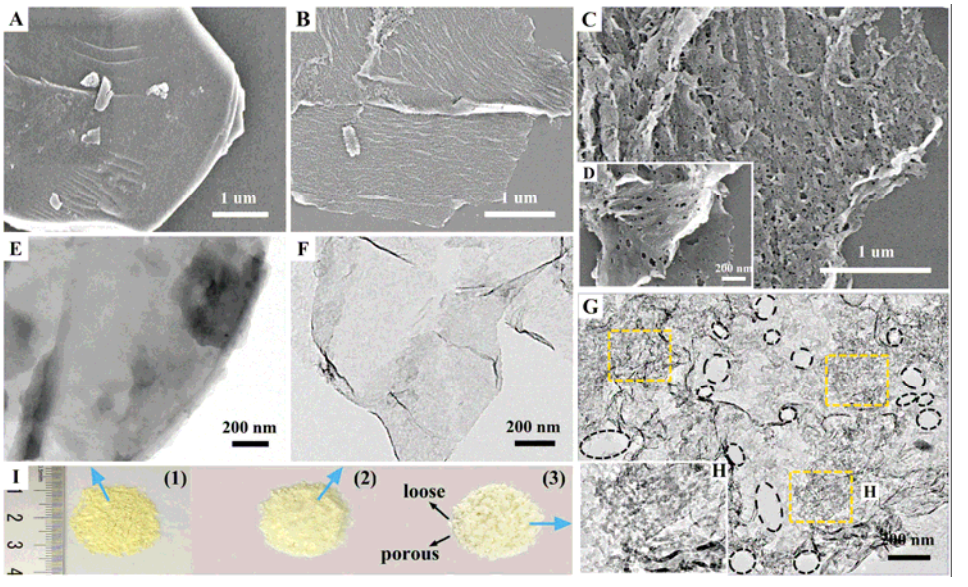

Fig. 5 SEM images of (A) CNB, (B) CNS, and (C) CNHS samples. TEM images of (E) CNB, (F) CNS, (G) and (H) CNHS samples, (I) photographs of (1) CNB, (2) CNS, and (3) CNHS. Reproduced with permission[20] (Copyright@2016, WILEY‐VCH Verlag GmbH & Co. KGaA, Weinheim)

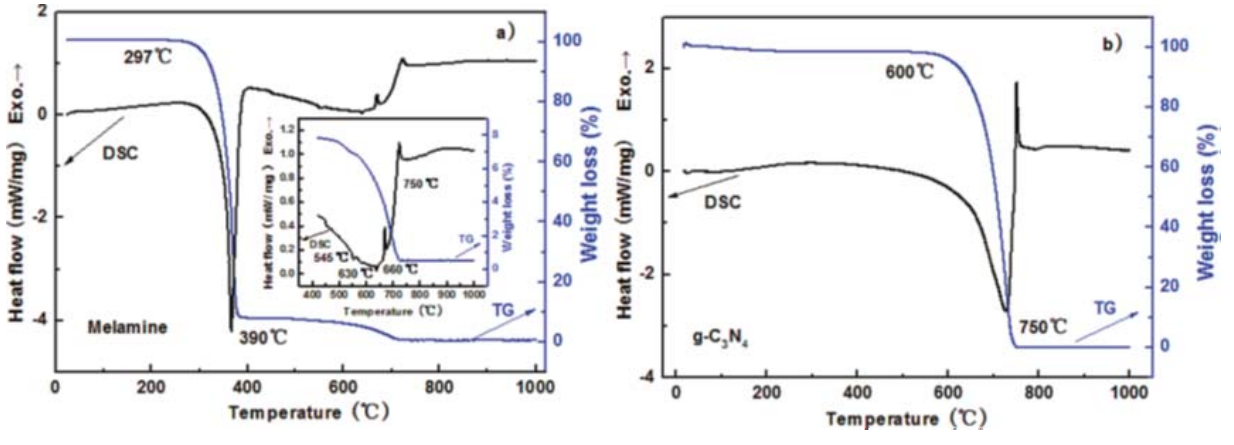

Fig. 6 TG-DSC thermograms for heating (a) melamine and (b) g-C_3N_4 obtained by heating melamine at 520 °C. Reproduced with permission[21] (Copyright © 2009, American Chemical Society)

was achieved via soft-chemical method. It found out that the samples stayed stable at temperatures up to 550 °C, suggesting a stable construction from heptazine-base units in the materials. Komatsu *et al.*[42] prepared g-C_3N_4 by polycondensation/pyrolysis of several tris-s-triazine derivatives, which were prepared from melamine and thiocyanates. Thermogravimetry shows that all the samples exhibited high heat-resistance over 600 °C, and the heat resistance of g-C_3N_4 tended to decrease with an increase in the nitrogen content. According to the report of Shi *et al.*,[47] g-C_3N_4 was synthesized by directly heating guanidine hydrochloride at different temperatures in air. Based on TG-DSC curve, the weight of g-C_3N_4 decreased rapidly between 600 and 700 °C, and decomposed totally at 700 °C. Yuan *et al.*[45] reported a high-yield synthesis of g-C_3N_4 by heating melamine powders under vacuum at temperatures between 450 and 650 °C. The samples obtained at 550-650 °C did not start to decompose until 640 °C. The high thermal stability of g-C_3N_4 features its various applications, as a heterogeneous organic catalyst, at operating temperature below 500 °C. High thermal stability also allows its easy removal by simply increasing the calcination temperature beyond 600 °C, thus favoring its utilization as confinement templates, structuring agents or nitrogen sources for synthesizing a refined carbon nanostructure or metal nitride nanostructures with continuously adjustable compositions.

3.1.2 Chemical stability

Besides, g-C_3N_4 also exhibits a great chemical stability. g-C_3N_4 possesses optimized van der Waals interactions between the layers, as a result, it is insoluble in most solvents, such as water, acid and many organic solvents.[48,49] However, treating g-C_3N_4 in molten alkali metal hydroxides or $KMnO_4$ results in a hydrolysis of its structure. However, treating g-C_3N_4 in concentrated acids leads to a colloidal dispersion. According to the report of Zhang *et al.*,[50] acids

did not chemically disintegrate g-C_3N_4. When treated in the concentrated-acid solvents at room temperature, g-C_3N_4 formed some dispersed nanosheets without destroying their layer structure.

3.2 Optical and photoelectrochemical properties

g-C_3N_4 possesses certain decisive optical properties, which have been studied by means of experimental characterizations and theoretical calculations. g-C_3N_4 has been used in various photochemistry-related areas, such as ultraviolet-visible absorption, photoluminescence and electrochemiluminescence.

As an inorganic semiconductor, g-C_3N_4 has a typical absorption bandgap adsorption at ~420 nm (Fig. 7).[51] In fact, this medium bandgap can be confirmed by the yellow color of g-C_3N_4, and the results are in consistence with previous reports.[52,53] It is also worth noting that some modification strategies can affect the absorption edge of g-C_3N_4, such as Fe, S, B doping[54,55] and copolymerization by barbituric acid.[56]

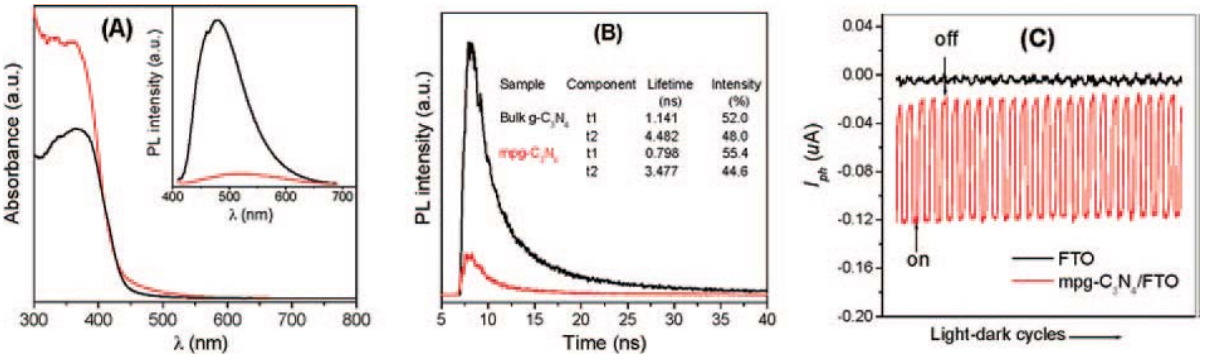

Fig. 7 (a) Diffuse reflectance absorption spectrum and photoluminescence (PL) spectrum (inset) under 420 nm excitation, and (b) time-resolved PL spectrum monitored at 525 nm under 420 nm excitation at 298 K for bulk g-C_3N_4 (black) and mpg-C_3N_4 (red). (c) Periodic on/off photocurrent I_{ph} response of mpg-C_3N_4 electrode in 0.5 M Na_2SO_4 under zero bias in a standard two electrode photoelectrochemical cell. Reproduced with permission [52] (Copyright © 2009, American Chemical Society)

In the report of Tahir *et al.*,[39] they researched the optical properties of bulk g-C_3N_4 (GCN) and g-C_3N_4 nanofibers (GCNNFs). GCN has a bandgap at 2.67 eV, while GCNNF has a bandgap at 2.80 eV. The slight blue shift by 0.13 eV is due to the more perfect packing, electronic coupling and quantum confinement effect that shift conduction and valence band edges.[39] Meanwhile, PL intensity of GCN is higher than that of GCNNF, which indicates the slow recombination rate of photogenerated electrons and holes. The decrease of PL intensity is caused by the defects in the crystal structure that reduces the strength of fluorescence peaks. These defects are the recombination centers for electrons and holes generated during photocatalysis. Therefore, a decrease in the number of defects in GCNNF ultimately increases its photocatalytic performance.

g-C_3N_4 has been employed in photoelectric conversion systems (photoelectrochemical cells *etc.*) because of its favorable electronic band structure.[57] Besides, in photoelectrochemical cells, g-C_3N_4's band gap can be adjusted by changing its morphology or doping. Also, photoelectrochemical cells can operate stably in O_2 due to the excellent chemical and thermal stability of g-C_3N_4.

3.3 Electrochemical properties

g-C_3N_4 can be used as electrocatalysts for various electrocatalytic reactions, such as oxygen reduction reaction (ORR) and hydrogen evolution reaction (HER).[58,59] g-C_3N_4 can provide a higher electrocatalytic activity than pure carbon,[60] which makes it become more attractive towards electrocatalysis. This is because g-C_3N_4 possesses pyridinic N atoms, which can accept electrons and serve as reaction active sites.[49,61] However, the performance and applications of g-C_3N_4 in electrochemical reactions are restricted by its poor conductivity and electron transportation. Zheng *et al.*[62] theoretically revealed that the low ORR catalytic activity of pure g-C_3N_4 is through an unfavorable 2e$^-$ pathway. While in the g-C_3N_4@carbon composite, a nearly 100% of selectivity for 4e-ORR pathway could be achieved in alkaline aqueous solutions. Recently, it has been demonstrated that the electrocatalytic activities of g-C_3N_4 can be significantly enhanced by coupling with other conductive supports to improve electron transfer. As a result, tremendous efforts have been made to explore more strategies to achieve new-generation g-C_3N_4-based electrocatalysts with higher conductivity and electrochemical performance.

4. Energy storage of g-C_3N_4

4.1 Photocatalytic hydrogen production

Hydrogen has been regarded as a clean energy source without consuming fossil fuels. Photocatalytic water splitting by employing semiconductor photocatalysts and solar energy is a promising approach to generate hydrogen energy. The choice of photocatalyst is vital for achieving ideal hydrogen production performance. Various kinds of photocatalysts have been explored in hydrogen evolution

reaction (HER), such as metal oxides,[63,64] metal nitrides,[65] metal sulfides[66] and metal phosphides[67] or their mixed solid solutions.[68,69] Besides these materials, g-C_3N_4 has been considered as an efficient photocatalyst because of its structural and electronic properties.[48] g-C_3N_4 possesses an appropriate bandgap and high specific surface area, therefore, it can promote the utilization of visible light and increase the electron transport, which will then promotes the photocatalytic hydrogen production.[70,71]

Maeda *et al.*[72] studied the performance of g-C_3N_4 as a nonmetallic photocatalyst for HER and OER under both ultraviolet (UV) and visible light. It indicated that g-C_3N_4 catalyst exhibited favorable performance for HER and oxygen evolution reaction (OER) due to a proper electron donor or acceptor. Zhang *et al.*[73] used a facile one-step synthesis process to prepare g-C_3N_4 as photocatalysts. The porous structure with increased specific surface area and pore volume helped g-C_3N_4 achieve a better hydrogen production activity.

However, the photocatalytic efficiency of pristine g-C_3N_4 is still not satisfactory. As a result, many researchers have employed other strategies to promote its photocatalytic properties. For example, g-C_3N_4 could be complexed with other electron-rich nanocomposites.[74] For example, g-C_3N_4 was complexed with nitrogen-doped graphene to catalyze HER.[60] This hybrid catalyst exhibited desirable HER activities due to its intrinsic chemical and electronic coupling. She *et al.*[75] confirmed that a small amount of α-Fe_2O_3 nanosheets formed 2D hybrid with g-C_3N_4, which exhibited an all-solid-state Z-scheme junction. The hybrid achieved a high H_2 evolution rate because the Z-scheme junction could suppress the recombination of electron-hole pairs as well as promote the overall water splitting without any sacrificial donor. Hou *et al.*[76] successfully constructed MoS_2/g-C_3N_4 nanojunctions, which exhibited enhanced photocatalytic HER activities under visible light compared with bare MoS_2 and g-C_3N_4. Besides, they also found that other layered transition metal dichalcogenides (for example, WS_2) promoted HER rates after complexed with g-C_3N_4. Besides, noble metal Pt is also a good choice of cocatalyst, however the high cost greatly limits its application. Li *et al.*[22] anchored isolated single Pt atoms on g-C_3N_4 with a high dispersion and stability to form a co-catalyst. It was found that Pt-CN remarkably enhanced the photocatalytic hydrogen evolution activity as well as achieved the maximum utilization of Pt atoms to reduce the cost.

On the other hand, doping selected heteroatoms is an efficient way to modify its electronic properties.[56,77] Some non-metallic elements, such as boron (B), fluorine (F), phosphor (P) and sulfur (S) are often introduced into g-C_3N_4 to modify its electronic structure and improve its photocatalytic activity.[1] Using P doping and thermal exfoliation, Ran *et al.*[78] successfully prepared porous P-doped g-C_3N_4 nanosheets. This photocatalyst showed a high visible-light photocatalytic hydrogen production rate. After P doping, the intrinsic bandgap of g-C_3N_4 was narrowed from 2.98 to 2.66 eV, and the empty midgap states (-0.16 V *vs.* SHE) induced by P doping was favorable for promoting the visible light absorption of P doped g-C_3N_4 nanosheets (PCN). In another paper, P doped g-C_3N_4 was prepared by a thermally induced copolymerization method.[79] The HER rate of P doped g-C_3N_4 reached 50.6 mmol h^{-1}, because P atoms changed the electronic structure of g-C_3N_4 and suppressed the recombination of charge carriers. Lan *et al.*[13] synthesized Br doped g-C_3N_4 for hydrogen evolution. By doping Br, the CNU-$Br_{0.1}$ showed more than two times higher HER rates than pure CNU sample. Some metallic elements also introduced free electrons to g-C_3N_4 to modify its electronic structure as well as provide organic-metal hybrid. Thang *et al.*[80] investigated cobalt (II) phosphide hydroxide co-doped g-C_3N_4 (Co-P/C_3N_4) for the hydrogen production. Results showed that the hydrogen production rate of Co-P/C_3N_4 was 14 times higher than g-C_3N_4.[80] Combining doped g-C_3N_4 with other photocatalyst can further promote their photocatalytic activity. Chen *et al.*[81] prepared a novel photocatalyst of Co-g-C_3N_4/MoS_2 by coupling Co-doped g-C_3N_4 and MoS_2 nanosheets. The photocatalytic activity of the catalyst was better than g-C_3N_4/MoS_2 and Co-g-C_3N_4, which was mainly due to the formation of a 2D heterojunction, promoted charge carrier transport, suppressed recombination of charge carriers, and increased light absorption.[81]

Table 1. HER performance of typical g-C_3N_4-based photocatalyst.

Materials	Application	HER rate	Ref
g-C_3N_4 powder/Pt	water reduction	7.3 μmol h^{-1}	[73]
porous g-C_3N_4	water splitting	0.25 μmol h^{-1}	[74]
α-Fe_2O_3/g-C_3N_4	water splitting	3×10^4 μmol g^{-1} h^{-1}	[76]
MoS_2/g-CN	water splitting	20.6 mmol h^{-1}	[77]
Pt-CN	water splitting	300 μmol h^{-1}	[22]
P doped g-C_3N_4	water splitting	1596 μmol g^{-1} h^{-1}	[79]
P doped g-C_3N_4	water reduction/ photodegradation of RhB	50.6 μmol h^{-1}	[80]
Br-modified g-C_3N_4	water reduction	48 μmol h^{-1}	[13]
Co-P/C_3N_4	water splitting	386.8 μmol g^{-1}	[81]
Co-g-C_3N_4/MoS_2	water reduction/ photodegradation of RhB	5411 μmol g^{-1} h^{-1}	[82]

4.2 Oxygen reduction reactions in fuel cells

Fuel cells attract great interest for offering cleaner and more sustainable energy. At present, the practical applications of fuel cells are restricted by the high cost of Pt catalyst and the sluggish kinetics of ORR.[14,82] Nitrogen-containing carbon materials, such as g-C_3N_4, are worthy investigating because they provide sufficient active sites for ORR.[1,83,84] However, the electrocatalytic performance of g-C_3N_4 is restricted by its poor electron transfer. To solve this problem, one strategy

is to use conductive carbon materials as support to improve the electron accumulation, thus to enhance the electrocatalytic performance. Lyth *et al.*[58] used g-C_3N_4 as a catalyst for oxygen reduction, and they found out that although the electrocatalytic activity of g-C_3N_4 was better than pure carbon, the current densities were pretty low, which possibly was due to its low surface area. It was found that the current densities increased by mixing C_3N_4 with carbon black.

Yang *et al.*[85] fabricated graphene-based C_3N_4 (G-CN) nanosheets by nanocasting. The G-CN nanosheets possessed a high nitrogen content and a high specific surface area and showed promoted electrical conductivities.[85] As a result, the G-CN nanosheets exhibited excellent electrocatalytic activity for ORR. Macroporous g-C_3N_4/C was prepared by using silica microspheres as hard templates.[14] This hybrid catalyst exhibited outstanding activities towards ORR in fuel cells, and was comparable with commercial Pt/C.[14] Liu *et al.*[15] doped Co into g-C_3N_4 polymer and supported it on graphene as a catalyst for ORR in alkaline fuel cells (Fig. 8). The experimental results showed that ORR catalyzed by Co-g-C_3N_4 mainly occurred in a four-electron pathway. The high ORR activity was attributed to the sufficient Co-N_x active sites and fast electron transport.[15]

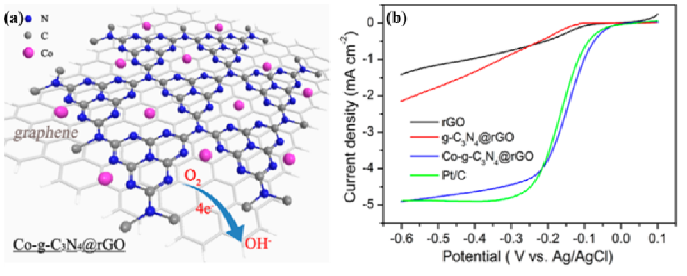

Fig. 8 (a) Schematic illustration of Co-g-C_3N_4/graphene; (b) RDE curves of four samples with a sweep rate of 5 mV s^{-1} at 1600 rpm in O_2-saturated 0.1 M KOH. Reproduced with permission [15] (Copyright © 2013, American Chemical Society)

Apart from carbon-based materials, some metals are also investigated to complex with g-C_3N_4 to achieve a better ORR performance. For example, Kundu *et al.*[59] reported a facile synthesis of porous gold aerogel supported on carbon nitride (Au-aerogel-CN_x). Results showed that four-electron ORR process was dominant at the catalysts in both alkaline and acidic media, and the excellent ORR performance was due to the synergistic effects between porous Au-aerogel-CN_x.[59] Zheng *et al.*[86] designed and synthesized a series of g-C_3N_4 coordinated transition metals as catalysts for oxygen electrode reactions. After theoretical calculation and experimental measurements of a Co-C_3N_4 catalyst, it was found that the high ORR activity was ascribed to the Co-N_2 coordination.[86]

It can be seen that g-C_3N_4 shows promising activity towards photocatalytic hydrogen evolution. Especially, when combined with conductive supports (such as mesoporous carbon or graphene), g-C_3N_4 can exhibit highly efficient ORR activity, which will be beneficial for the development of fuel cells. Although g-C_3N_4 has a great potential in various applications, the correlations between the g-C_3N_4 structure and its catalytic activity are still not clear. Current research basically focuses on the performance rather than the mechanism. For future studies, powerful theoretical calculation is needed to understand the physicochemical properties of carbon nitride and to clarify the relationship of nanostructure and catalytic kinetics. Besides, in current research, the combination of g-C_3N_4 and other materials has achieved promising performances, but the inherit mechanism is still needed to be found out.

Table 2. Typical g-C_3N_4-based catalyst ORR performance.

Materials	Application	Onset Potential (V)	Current Density (mA cm^{-2})	Ref
g-C_3N_4/CB	fuel cells	0.76	2.21	[59]
Graphene-C_3N_4	fuel cells	-	7.3	[86]
g-C_3N_4/C	fuel cells	-0.14	4.3	[14]
Co-g-C_3N_4@ graphene	fuel cells	-0.03	4.9	[15]
Au-aerogel-CN_x	-	0.92	10	[60]
Co-C_3N_4/CNT	-	0.9 V	5 mA cm^{-2}	[87]

4.3 Li-based battery

Because of the relatively high specific energy and good stability, some Li-based batteries, such as Li-ion battery, Li-O_2 battery and Li-S battery have attracted tremendous interests for their potential applications in electric vehicles. However, the practical applications of these batteries are restricted by the sluggish kinetics of the reactions on the electrodes. In order to solve this problem, efficient catalyst should be developed and employed. g-C_3N_4 may provide more active sites for the electrode reactions due to its high nitrogen content.[87,88] Still, g-C_3N_4 is limited by the low electronic conductivity. Therefore, some electronic conductive materials should be used to increase electrons accumulated on g-C_3N_4 surface.[87]

Hou *et al.*[89] prepared a N-doped graphene/porous g-C_3N_4 nanosheets supporting layered-MoS_2 hybrid as Li-ion battery anodes. MoS_2 nanosheets were dispersed uniformly on the matrix to form a multilayered structure.[89] The hybrid catalyst shows excellent cycling stability, high rate capability and large capacity due to the special structure. Yin *et al.*[90] anchored SnS_2 on g-C_3N_4 nanosheets to synthesize a composite electrode for Li-ion batteries. The large surface area provided more active sites and promoted the charge transfer. Besides, the synergistic effect between g-C_3N_4 nanosheets and SnS_2 lowered the charge-transfer resistance, which was in favor of the alloying reaction between metallic Sn and Li^+. As a result, the catalyst delivered a high discharge capacity with a high coulombic efficiency of over 99.9%, and it also achieved a high specific capacity retention rate. g-C_3N_4@carbon papers

(GCN@CP) were prepared via a facile in situ method to improve the electronic conductivity of g-C_3N_4 and obtained a high nitrogen content.[18] When employed as cathodes for Li-O_2 batteries, GCN@CP exhibited favorable electrocatalytic performance toward ORR and OER in nonaqueous electrolytes, showing good rate capability and cyclic stability. In another paper, Luo *et al.*[91] synthesized a free-standing graphene@g-C_3N_4 (G@CN) composite cathode for Li-O_2 batteries. During the reaction process, g-C_3N_4 nanosheets acted as electrocatalysts while graphene nanosheets accommodated Li_2O_2 and improved the electron transfer.[91] As a result, the G@CN electrocatalyst showed a favorable cyclic stability with a high round-trip efficiency. Zhao *et al.*[92] synthesized single-atom Pt catalyst supported on holey ultrathin g-C_3N_4 nanosheets (Pt-CNHS) to serve as cathode in Li-O_2 battery (Fig. 9). Li-O_2 batteries utilizing Pt-CNHS showed much higher discharge specific capacities than those with pure CNHS.

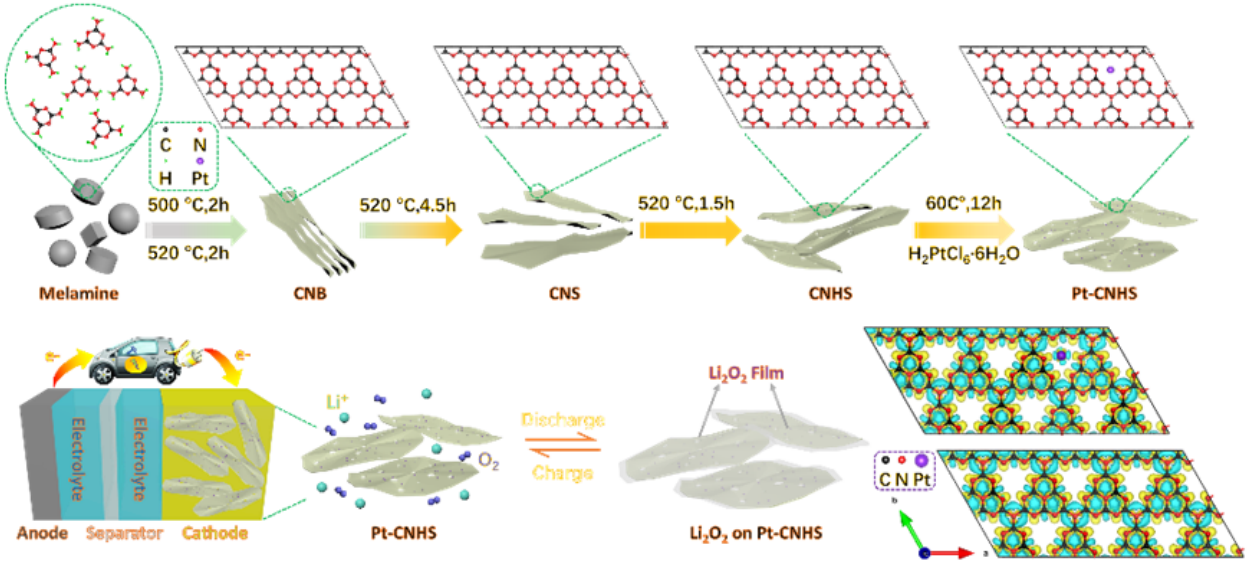

Fig. 9 Schematic illustration of the synthesis and reaction mechanism of Pt-CNHS. Reproduced with permission[93] (Copyright@2019, Elsevier Ltd.)

The assembled batteries using Pt-CNHS as catalyst could deliver a 17059.5 mAh g^{-1} discharge capacity, while that of pure CNHS was only 5890.1 mAh g^{-1}. CNHS with porous structure promoted the mass transport and electrolyte wetting, as well as accommodated Li_2O_2. Single-atom Pt was also in favor of the efficient interfacial mass transfer due to its high electrical conductivity. Meng *et al.*[19] used g-C_3N_4 nanosheets as a sulfur anchoring material in Li-S batteries. The as-prepared g-C_3N_4 nanosheets possessed a high nitrogen (N) content of 56 wt% and a high specific surface area of 209.8 m^2 g^{-1}, which were in favor of the loading of lithium polysulfides. As a result, the GCN/S delivered good electrochemical performances at the initial and 750th cycle.[19] 3D light-weight and porous C_3N_4 nanosheets@reduced graphene oxide (PCN@rGO) network was prepared to solve the shuttle effect in Li-S batteries.[93] The PCN@rGO network anchored polysulfides by strong chemical adsorption as well as promoted electron and mass transfer.[93] As a result, the PCN@rGO-S cathode showed superior rate capability and ultra-long cycling stability. Zhang *et al.*[94] synthesized a 3D porous sulfur/graphene@g-C_3N_4 (S/GCN) hybrid sponge and applied it as a free-standing cathode for Li-S batteries. The N-sites in GCN provided a large amount of adhesion sites for polysulfides, achieving a "physical-chemical" dual-confinement for polysulfides. Moreover, the porous 3D graphene frameworks promoted electron/Li^+ transport and maintained good structure integrity. By using a microemulsion encapsulation method, S/GCN cathodes achieved a sulfur loading up to 82 wt%. Therefore, the S/GCN delivered a high specific capacity and excellent rate capability as well as alleviated anode corrosion issues.

5. Summary and outlook

In summary, this review presents an overview of g-C_3N_4 and g-C_3N_4-based materials, focusing on the synthesis methods, properties and applications in energy storage. The unique properties and wide applications prove that g-C_3N_4 is promising for efficient energy storage. Therefore, the research of g-C_3N_4-based composite for energy storage and conversion will continue to accelerate in the near future.

g-C_3N_4 exhibits great activities for photocatalytic hydrogen production in water splitting. Besides, when blending with other electrocatalyst, g-C_3N_4 can become highly efficient for ORR catalyzing. Therefore, the applications of g-C_3N_4 can be extended to fuel cells and some Li-based secondary batteries. To date, some researchers have attempted to make g-C_3N_4 based materials serve as catalysts in secondary batteries and achieved satisfying results. Still, the studies are preliminary, and more efforts should be focused on the internal reaction process during discharge and charge cycle. In general, considerable progress has been achieved regarding g-C_3N_4, but the studies are still not complete. The relationship between the

g-C_3N_4 unique structure and catalytic activity is still not clear. There are still many opportunities for further research efforts. Accordingly, more studies are needed to figure out the structural and electronic properties of g-C_3N_4.

As g-C_3N_4 related research develops, an urgent and realistic question is raised: what else can we continue to work on g-C_3N_4-based material presently? After reviewing the research works in the past, we believe that the following problems should be solved in the future studies:(1) New synthesis process for g-C_3N_4 should be proposed. As we introduced in this review, g-C_3N_4 is commonly prepared from the condensation of nitrogen rich precursors, which can be polymerized into various mediates. In order to improve the catalytic activity of g-C_3N_4, exploiting new methods to prepare the g-C_3N_4 with a higher crystalline quality is of great importance. (2) A more comprehensive understanding of the reaction mechanism is necessary for promoting the design and performance of g-C_3N_4 based catalysts. The charge carrier transfer mechanism, the thermodynamics and kinetics of surface reactions are worth studying. In order to realize the understanding of mechanism, some powerful tools, such as in-situ characterization techniques and theoretical calculation may be of great importance. (3) Apart from the research of sole g-C_3N_4, combining it with other novel catalysts may be a path towards more efficient energy storage strategies. It's important that researchers should try to design a g-C_3N_4 based composite rather than simply find one. Therefore, the understanding of g-C_3N_4 and other novel materials is vital for the new catalyst. In a word, there are enormous opportunities regarding g-C_3N_4 and g-C_3N_4-based materials, but this may require the unremitting efforts of worldwide researchers.

Acknowledgements

This work was supported by the National Natural Science Foundation of China (No. 51672162), Shenzhen Science and Technology Plan Projects (No. JCYJ20170818105351600).

Supporting information

Not applicable

Conflict of interest

There are no conflicts to declare.

References

[1] Y. Zheng, J. Liu, J. Liang, M. Jaroniec and S. Z. Qiao, *Energy Environ. Sci.*, 2012, **5**, 6717-6731, doi: 10.1039/c2ee03479d.

[2] M. Kawaguchi, S. Yagi and H. Enomoto, *Carbon*, 2004, **42**, 345-350, doi: 10.1016/j.carbon.2003.11.004.

[3] E. Kroke and M. Schwarz, *Coord. Chem. Rev.*, 2004, **248**, 493-532, doi: 10.1016/j.ccr.2004.02.001.

[4] K. Kailasam, J. D. Epping, A. Thomas, S. Losse, H. Junge, *Energy Environ. Sci.*, 2011, **4**, 4668-4674, doi: 10.1039/c1ee02165f.

[5] V. N. Khabashesku, J. L. Zimmerman and J. L. Margrave, *Chem. Mater.*, 2000, **12**, 3264-3270, doi: 10.1021/cm000328r.

[6] E. G. Gillan, *Chem. Mater.*, 2000, **12**, 3906-3912, doi: 10.1021/cm000570y.

[7] J. L. Zimmerman, R. Williams, V. N. Khabashesku and J. L. Margrave, *Nano Lett.*, 2001, **1**, 731-734, doi: 10.1021/nl015626h.

[8] Y. Gong, M. Li, Y. Wang, *ChemSusChem*, 2015, **8**, 931-946, doi: 10.1002/cssc.201403287.

[9] E. Kroke, M. Schwarz, E. Horath Bordon, P. Kroll, B. Noll and A. D. Norman, *New J. Chem.*, 2002, **26**, 508-512, doi: 10.1039/b111062b.

[10] J. Sehnert, K. Baerwinkel and J. Senker, *Journal of Physical Chemistry B*, 2007, **111**, 10671-10680, doi: 10.1021/jp072001k.

[11] W. J. Ong, L. L. Tan, Y. H. Ng, S. T. Yong and S. P. Chai, *Chem. Rev.*, 2016, **116**, 7159-7329, doi: 10.1021/acs.chemrev.6b00075.

[12] Q. Han, B. Wang, J. Gao, Z. H. Cheng, Y. Zhao, Z. P. Zhang and L. T. Qu, *ACS nano*, 2016, **10**, 2745-2751, doi: 10.1021/acsnano.5b07831.

[13] Z. A. Lan, G. G. Zhang and X. C. Wang, *Appl. Catal. B-Environ.*, 2016, **192**, 116-125, doi: 10.1016/j.apcatb.2016.03.062.

[14] J. Liang, Y. Zheng, J. Chen, J. Liu, D. Hulicova-Jurcakova, M. Jaroniec and S. Z. Qiao, *Angewandte Chemie International Edition*, 2012, **51**, 3892-3896, doi: 10.1002/anie.201107981.

[15] Q. Liu and J. Y. Zhang, *Langmuir : the ACS journal of surfaces and colloids*, 2013, **29**, 3821-3828, doi: 10.1021/la400003h.

[16] J. W. Fu, B. C. Zhu, C. J. Jiang, B. Cheng, W. You and J. G. Yu, *Small*, 2017, **13**, 1603938, doi: 10.1002/smll.201603938.

[17] K. Wang, Q. Li, B. S. Liu, B. Cheng, W. K. Ho and J. G. Yu, *Appl. Catal. B-Environ.*, 2015, **176-177**, 44-52, doi: 10.1016/j.apcatb.2015.03.045.

[18] J. Yi, K. M. Liao, C. F. Zhang, T. Zhang, F. J. Li and H. S. Zhou, *ACS Appl. Mater. Interfaces*, 2015, **7**, 10823-10827, doi: 10.1021/acsami.5b01727.

[19] Z. Meng, Y. Xie, T. W. Cai, Z. X. Sun, K. M. Jiang and W. Q. Han, *Electrochim. Acta*, 2016, **210**, 829-836, doi: 10.1016/j.electacta.2016.06.032.

[20] Y. F. Li, R. X. Jin, Y. Xing, J. Q. Li, S. Y. Song, X. C. Liu, M. Li and R. C. Jin, *Adv. Energy Mater.*, 2016, **6**, 1601273, doi: 10.1002/aenm.201601273.

[21] S. C. Yan, Z. S. Li and Z. G. Zou, *Langmuir: the ACS journal of surfaces and colloids*, 2009, **25**, 10397-10401, doi: 10.1021/la900923z.

[22] X. G. Li, W. T. Bi, L. Zhang, S. Tao, W. S. Chu, Q. Zhang, Y. Luo, C. Z. Wu and Y. Xie, *Adv. Mater.*, 2016, **28**, 2427, doi: 10.1002/adma.201505281.

[23] Y. P. Yuan, W. T. Xu, L. S. Yin, S. W. Cao, Y. S. Liao, Y. Q. Tng and C. Xue, *Int. J. Hydrogen Energ.*, 2013, **38**, 13159-13163, doi: 10.1016/j.ijhydene.2013.07.104.

[24] L. J. Ye and S. J. Chen, *Appl. Surf. Sci.*, 2016, **389**, 1076-1083, doi: 10.1016/j.apsusc.2016.08.038.

[25] F. Dong, Z. W. Zhao, T. Xiong, Z. L. Ni, W. D. Zhang, Y. J. Sun and W. K. Ho, *ACS Appl. Mater. Interfaces*, 2013, **5**, 11392-11401, doi: 10.1021/am403653a.

[26] K. Takanabe, K. Kamata, X. Wang, M. Antonietti, J. Kubota and K. Domen, *Physical Chemistry Chemical Physics*, 2010, **12**, 13020-13025, doi: 10.1039/c0cp00611d.

[27] X. Wang, K. Maeda, A. Thomas, K. Takanabe, G. Xin, J. M.

Carlsson, K. Domen and M. Antonietti, *Nat. Mater.*, 2009, **8**, 76-80, doi: 10.1038/nmat2317.

[28] A. Thomas, F. Goettmann and M. Antonietti, *Chem. Mater.*, 2008, **20**, 738-755, doi: 10.1021/cm702126j.

[29] J. H. Huang, W. Ho and X. C. Wang, *Chem. Commun.*, 2014, **50**, 4338-4340, doi: 10.1039/c3cc48374f.

[30] X. Li, A. F. Masters and T. Maschmeyer, *ChemCatChem*, 2015, **7**, 121-126, doi: 10.1002/cctc.201402567.

[31] M. Groenewolt and M. Antonietti, *Adv. Mater.*, 2005, **17**, 1789-1792, doi: 10.1002/adma.200401756.

[32] S. N. Talapaneni, G. P. Mane, A. Mano, C. Anand, D. S. Dhawale, T. Mori and A. Vinu, *ChemSusChem*, 2012, **5**, 700-708, doi: 10. 1002/cssc.201100626.

[33] Y. Fukasawa, K. Takanabe, A. Shimojima, M. Antonietti, K. Domen and T. Okubo, *Chem. Asian J.*, 2011, **6**, 103-109, doi: 10. 1002/asia.201000523.

[34] J. Xu, H. T. Wu, X. Wang, B. Xue, Y. X. Li and Y. Cao, *Physical Chemistry Chemical Physics*, 2013, **15**, 4510-4517, doi: 10. 1039/c3cp44402c.

[35] S. S. Park, S. W. Chu, C. F. Xue, D. Y. Zhao and C. S. Ha, *J. Mater. Chem.*, 2011, **21**, 10801-10807, doi: 10.1039/c1jm10849b.

[36] H. J. Yan, *Chem. Commun.*, 2012, **48**, 3430-3432, doi: 10.1039/c2cc00001f.

[37] H. Yang, K. L. Lv, J. J. Zhu, Q. Li, D. G. Tang, W. K. Ho, M. Li and S. A. C. Carabineiro, *Appl. Surf. Sci.*, 2017, **401**, 333-340, doi: 10.1016/j.apsusc.2016.12.238.

[38] K. K. Han, C. C. Wang, Y. Y. Li, M. M. Wan, Y. Wang and J. H. Zhu, *RSC Adv.*, 2013, **3**, 9465-9469, doi: 10.1039/c3ra40765a.

[39] M. Tahir, C. Cao, N. Mahmood, F. K. Butt, A. Mahmood, F. Idrees, S. Hussain, M. Tanveer, Z. Ali and I. Aslam, *ACS Appl. Mater. Interfaces*, 2014, **6**, 1258-1265, doi: 10.1021/am405076b.

[40] Q. Yu, S. Guo, X. Li and M. Zhang, *Mater. Technol.*, 2014, **29**, 172-178, doi: 10.1179/1753555714y.0000000126.

[41] X. J. She, H. Xu, Y. G. Xu, J. Yan, J. X. Xia, L. Xu, Y. H. Song, Y. Jiang, Q. Zhang and H. M. Li, *J. Mater. Chem. A*, 2014, **2**, 2563-2570, doi: 10.1039/c3ta13768f.

[42] T. Komatsu and T. Nakamura, *J. Mater. Chem.*, 2001, **11**, 474-478, doi: 10.1039/b005982j.

[43] D. R. Miller, J. Wang and E. G. Gillan, *J. Mater. Chem.*, 2002, **12**, 2463-2469, doi: 10.1039/b109700h.

[44] Y. J. Cui, J. S. Zhang, G. G. Zhang, J. H. Huang, P. Liu, M. Antonietti and X. C. Wang, *J. Mater. Chem.*, 2011, **21**, 13032-13039, doi: 10.1039/c1jm11961c.

[45] Y. Yuan, L. Zhang, J. Xing, M. I. Utama, X. Lu, K. Du, Y. Li, X. Hu, S. Wang, A. Genc, R. Dunin Borkowski, J. Arbiol and Q. Xiong, *Nanoscale*, 2015, **7**, 12343-12350, doi: 10.1039/c5nr02905h.

[46] M. Kawaguch, *Chem. Mater.*, 1995, **7**, 257-264, doi: 10.1021/cm00050a005,.

[47] L. Shi, L. Liang, F. X. Wang, J. Ma and J. M. Sun, *Catal. Sci. Technol.*, 2014, **4**, 3235-3243, doi: 10.1039/c4cy00411f.

[48] Y. Wang, X. Wang and M. Antonietti, *Angewandte Chemie International Edition*, 2012, **51**, 68-89, doi: 10.1002/anie.201101182.

[49] J. Q. Wen, J. Xie, X. B. Chen and X. Li, *Appl. Surf. Sci.*, 2017, **391**, 72-123, doi: 10.1016/j.apsusc.2016.07.030.

[50] Y. Zhang, A. Thomas, M. Antonietti and X. Wang, *J. Am. Chem. Soc.*, 2009, **131**, 50-51, doi: 10.1021/ja808329f.

[51] X. C. Wang, K. Maeda, X. F. Chen, K. Takanabe, K. Domen, Y. D. Hou, X. Z. Fu and M. Antonietti, *J. Am. Chem. Soc.*, 2009, **131**, 1680-1681, doi: 10.1021/ja809307s.

[52] M. Deifallah, P. F. McMillan and F. Cora, *J. Phys. Chem. C*, 2008, **112**, 5447-5453, doi: 10.1021/jp711483t.

[53] J. Wang, D. R. Miller and E. G. Gillan, *Chem. Commun.*, 2002, 2258-2259, doi: 10.1039/b207041c.

[54] Y. Wang, Y. Di, M. Antonietti, H. R. Li, X. F. Chen and X. C. Wang, *Chem. Mater.*, 2010, **22**, 5119-5121, doi: 10.1021/cm1019102.

[55] G. Liu, P. Niu, C. H. Sun, S. C. Smith, Z. G. Chen, G. Q. Lu and H. M. Cheng, *J. Am. Chem. Soc.*, 2010, **132**, 11642-11648, doi: 10. 1021/ja103798k.

[56] J. S. Zhang, X. F. Chen, K. Takanabe, K. Maeda, K. Domen, J. D. Epping, X. Z. Fu, M. Antonietti and X. C. Wang, *Angewandte Chemie International Edition*, 2010, **49**, 441-444, doi: 10.1002/anie.200903886.

[57] Y. J. Zhang and M. Antonietti, *Chem. Asian J.*, 2010, **5**, 1307-1311, doi: 10.1002/asia.200900685.

[58] S. M. Lyth, Y. Nabae, S. Moriya, S. Kuroki, M. Kakimoto, J. Ozaki and S. Miyata, *J. Phys. Chem. C*, 2009, **113**, 20148-20151, doi: 10.1021/jp907928j.

[59] M. K. Kundu, T. Bhowmik and S. Barman, *J. Mater. Chem. A*, 2015, **3**, 23120-23135, doi: 10.1039/c5ta06740e.

[60] Y. Zheng, Y. Jiao, Y. Zhu, L. H. Li, Y. Han, Y. Chen, A. Du, M. Jaroniec and S. Z. Qiao, *Nat. Commun.*, 2014, **5**, 3783, doi: 10.1038/ncomms4783.

[61] J. Liu, H. Wang and M. Antonietti, *Chem. Soc. Rev.*, 2016, **45**, 2308-2326, doi: 10.1039/c5cs00767d.

[62] Y. Zheng, Y. Jiao, J. Chen, J. Liu, J. Liang, A. J. Du, W. M. Zhang, Z. H. Zhu, S. C. Smith, M. Jaroniec, G. Q. Lu and S. Z. Qiao, *J. Am. Chem. Soc.*, 2011, **133**, 20116-20119, doi: 10.1021/ja209206c.

[63] H. F. Shen, Y. J. Lu, Y. M. Wang, Z. D. Pan, G. Z. Cao, X. H. Yan and G. L. Fang, *J. Adv. Ceram.*, 2016, **5**, 298-307, doi: 10.1007/ s40145-016-0203-3.

[64] I. Fujimoto, N. Wang, R. Saito, Y. Miseki, T. Gunji and K. Sayama, *Int. J. Hydrogen Energ.*, 2014, **39**, 2454-2461, doi: 10.1016/j. ijhydene.2013.08.114.

[65] Z. X. Yin, Y. Sun, C. L. Zhu, C. Y. Li, X. T. Zhang and Y. J. Chen, *J. Mater. Chem. A*, 2017, **5**, 13648-13658, doi: 10.1039/c7ta02876h.

[66] S. Sun, T. Hisatomi, Q. Wang, S. S. Chen, G. J. Ma, J. Y. Liu, S. Nandy, T. Minegishi, M. Katayama and K. Domen, *ACS Catal.*, 2018, **8**, 1690-1696, doi: 10.1021/acscatal.7b03884.

[67] J. Yu, Q. Li, N. Chen, C. Y. Xu, L. Zhen, J. Wu and V. P. Dravid, *ACS Appl. Mater. Interfaces*, 2016, **8**, 27850-27858, doi: 10.1021/acsami.6b10552.

[68] Y. R. Li, J. Xu, Z. Y. Liu and H. Yu, *J. Mater. Sci-Mater. El.*, 2019, **30**, 11694-11705, doi: 10.1007/s10854-019-01529-0.

[69] F.E. Osterloh, *Chem. Mater.*, 2008, **20**, 35-54, doi: 10.1021/cm7024203.

[70] Z. Zhao, Y. Sun and F. Dong, *Nanoscale*, 2015, **7**, 15-37, doi: 10.1039/c4nr03008g.

[71] S. Cao and J. Yu, *J. Phys. Chem. Lett.*, 2014, **5**, 2101-2107, doi:

10.1021/jz500546b.

[72] K. Maeda, X. C. Wang, Y. Nishihara, D. L. Lu, M. Antonietti and K. Domen, *J. Phys. Chem. C*, 2009, **113**, 4940-4947, doi: 10.1021/jp809119m.

[73] Y. W. Zhang, J. H. Liu, G. Wu and W. Chen, *Nanoscale*, 2012, **4**, 5300-5303, doi: 10.1039/c2nr30948c.

[74] X. H. Li, J.S. Chen, X. Wang, J. Sun and M. Antonietti, *J. Am. Chem. Soc.*, 2011, **133**, 8074-8077, doi: 10.1021/ja200997a.

[75] X. J. She, J. J. Wu, H. Xu, J. Zhong, Y. Wang, Y. H. Song, K. Q. Nie, Y. Liu, Y. C. Yang, M.-T. F. Rodrigues, R. Vajtai, J. Lou, D. L. Du, H. M. Li and P. M. Ajayan, *Adv. Energy Mater.*, 2017, **7**, 1700025, doi: 10.1002/aenm.201700025.

[76] Y. Hou, A. B. Laursen, J. Zhang, G. Zhang, Y. Zhu, X. Wang, S. Dahl and I. Chorkendorff, *Angewandte Chemie International Edition*, 2013, **52**, 3621-3625, doi: 10.1002/anie.201210294.

[77] D. S. Geng, S. L. Yang, Y. Zhang, J. L. Yang, J. Liu, R. Y. Li, T. K. Sham, X. L. Sun, S. Y. Ye and S. Knights, *Appl. Surf. Sci.*, 2011, **257**, 9193-9198, doi: 10.1016/j.apsusc.2011.05.131.

[78] J. R. Ran, T. Y. Ma, G. P. Gao, X. W. Du and S. Z. Qiao, *Energy Environ. Sci.*, 2015, **8**, 3708-3717, doi: 10.1039/c5ee02650d.

[79] Y. J. Zhou, L. X. Zhang, J. J. Liu, X. Q. Fan, B. Z. Wang, M. Wang, W. C. Ren, J. Wang, M. L. Li and J. L. Shi, *J. Mater. Chem. A*, 2015, **3**, 3862-3867, doi: 10.1039/c4ta05292g.

[80] P. Q. Thang, K. Jitae, T. D. Nguyen, P. T. Huong, N. M. Viet and T. M. Al Tahtamouni, *Rendiconti Lincei. Scienze Fisiche e Naturali*, 2019, doi: 10.1007/s12210-019-00844-2.

[81] T. Chen, D. G. Yin, F. F. Zhao, K. K. Kyu, B. Q. Liu, D. W. Chen, K. X. Huang, L. L. Deng and L. Q. Li, *New J. Chem.*, 2019, **43**, 463-473, doi: 10.1039/c8nj04849e.

[82] B. C. H. Steele and A. Heinzel, *Nature*, 2001, **414**, 345-352, doi: 10.1038/35104620.

[83] R. Liu, D. Wu, X. Feng, K. Mullen, *Angewandte Chemie International Edition*, 2010, **49**, 2565-2569, doi: 10.1002/anie.200907289.

[84] W. Yang, T.-P. Fellinger and M. Antonietti, *J. Am. Chem. Soc.*, 2011, **133**, 206-209, doi: 10.1021/ja108039j.

[85] S. B. Yang, X. L. Feng, X. C. Wang and K. Mullen, *Angewandte Chemie International Edition*, 2011, **50**, 5339-5343, doi: 10.1002/anie.201100170.

[86] Y. Zheng, Y. Jiao, Y. Zhu, Q. Cai, A. Vasileff, L. H. Li, Y. Han, Y. Chen and S. Z. Qiao, *J. Am. Chem. Soc.*, 2017, **139**, 3336-3339, doi: 10.1021/jacs.6b13100.

[87] Y. Zheng, Y. Jiao, M. Jaroniec, Y. G. Jin and S. Z. Qiao, *Small*, 2012, **8**, 3550-3566, doi: 10.1002/smll.201200861.

[88] X. C. Wang, X. F. Chen, A. Thomas, X. Z. Fu and M. Antonietti, *Adv. Mater.*, 2009, **21**, 1609-1612, doi: 10.1002/adma.200802627.

[89] Y. Hou, J. Y. Li, Z. H. Wen, S. M. Cui, C. Yuan and J. H. Chen, *Nano Energy*, 2014, **8**, 157-164, doi: 10.1016/j.nanoen.2014. 06.003.

[90] L. X. Yin, R. L. Cheng, Q. Song, J. Yang, X. G. Kong, J. F. Huang, Y. Lin and H. B. Ouyang, *Electrochim. Acta*, 2019, **293**, 408-418, doi: 10.1016/j.electacta.2018.10.020.

[91] W. B. Luo, S. L. Chou, J. Z. Wang, Y. C. Zhai and H. K. Liu, *Small*, 2015, **11**, 2817-2824, doi: 10.1002/smll.201403535.

[92] W. Zhao, J. Wang, R. Yin, B. Li, X. S. Huang, L. L. Zhao and L. Qian, *J. Colloid Interf. Sci.*, 2020, **564**, 28-36, doi: 10.1016/j.jcis.2019.12.102.

[93] Y. Gong, C. P. Fu, G. P. Zhang, H. H. Zhou and Y. F. Kuang, *Electrochim. Acta*, 2017, **256**, 1-9, doi: 10.1016/j.electacta.2017.10.032.

[94] J. Zhang, J. Y. Li, W. P. Wang, X. H. Zhang, X. H. Tan, W. G. Chu and Y. G. Guo, *Adv. Energy Mater.*, 2018, **8**, 1702839, doi: 10.1002/aenm.201702839.

